ACS EARTH AND SPACE CHEMISTRY

http://pubs.acs.org/journal/aesccq

Article

Benzonaphthothiophene: Molecular Indicators for Thermal Maturity

Jiayang Li and Zhihuan Zhang*

Cite This: https://doi.org/10.1021/acsearthspacechem.2c00309

Read Online

ACCESS | Metrics & More | Article Recommendations

ABSTRACT: Benzonaphthothiophenes (BNTs) were firmly identified in coals by comparison with retention indices reported in the literature. The thermodynamic stabilities of BNTs were calculated by quantum chemical computations, and their stability sequence is as follows: [2,1]BNT > [2,3]BNT > [1,2]BNT. The BNT isomers are ubiquitous in coal samples from the Xihu Depression and the Ordos Basin. This study reveals the effects of thermal maturity on the distributions of BNTs in coals, where the relative abundances of [1,2]BNT and [2,3]BNT to [2,1]BNT were observed to be mainly controlled by thermal maturation conditions. Combining with theoretical calculations of thermodynamic stability, two benzonaphthothiophene maturity indicators, defined as BNTR-1 ([2,1]BNT/[2,3]BNT) and BNTR-2 ([2,1]BNT/([1,2]BNT + [2,3]BNT)), were proposed. Two preliminary calibrations of BNTR-1 and BNTR-2 against measured vitrinite reflectance (%Ro) were established, and the relationships are as follows: %Rc = 5.5 × BNTR-1/100 + 0.5 (%Ro >0.9) and %Rc = 15 × BNTR-2/100 + 0.5 (%Ro > 0.9), respectively. BNTR-1 and BNTR-2 have good correlations with the widely used molecular maturity parameters. The good correlations with vitrinite reflectance and maturity parameters suggest that BNTR-1 and BNTR-2 are useful indicators in evaluating the maturity for sedimentary organic matter at high levels of thermal stress. The accuracy of the BNT ratio ([2,1]BNT/[1,2]BNT) must be kept in mind when it is used as a migration tracer of oil generated at a high thermal maturation stage. There is no clear trend for the absolute concentrations of BNTs with increasing pristane/phytane and gammacerane/C_{30} hopane values, suggesting that the redox conditions and water salinity during deposition may have little influence on the generation of BNTs. This study can expand the understanding of the distribution and geochemical significance of complex sulfur-containing organic compounds in sedimentary organic matter.

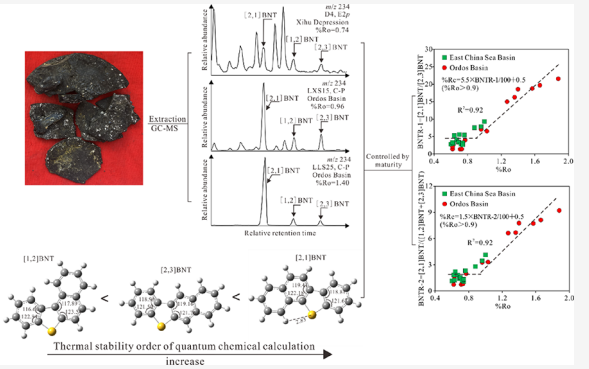

KEYWORDS: *benzonaphthothiophene, quantum chemical calculation, stability, thermal maturity, coal*

1. INTRODUCTION

Benzonaphthothiophenes are important organosulfur compounds in coal tar, coal liquids, shale oils, sedimentary rocks, and oils.[1−4] Much work has been achieved on their identification and occurrence in oils and application in tracking oil migration.[5−8] However, little is known about the distribution, controlling factor, and geochemical significance of benzonaphthothiophenes in sedimentary organic matter.

Two benzonaphthothiophene (BNT) isomers were first detected in coal liquids and shale oils by gas chromatography−mass spectrometry (GC−MS) analysis.[2] All three benzonaphthothiophene isomers (BNTs), i.e., benzo[*b*]naphtho[2,1-*d*]thiophene ([2,1]BNT), benzo[*b*]naphtho[1,2-*d*]thiophene ([1,2]BNT]), and benzo[*b*]naphtho[2,3-*d*]thiophene ([2,3]BNT), were identified by GC−MS.[9,10] By co-injection of authentic internal standards, Li et al.[3] firmly identified three benzonaphthothiophene isomers in lacustrine shales, marine carbonates, and crude oils and reported their retention indices, which now can be used in BNTs identification in other laboratories. Benzonaphthothiophenes were detected in light oils, condensates,[5,7,11] and sedimentary rocks.[12] However, less work has been done on the distribution patterns of benzonaphthothiophenes in coals.

There are few studies on the genesis and formation mechanism of BNTs. Hughes[13] suggested that some aromatic compounds with thiophenic-type ring systems in kerogen are probably precursors for thiophene compounds. Douglas and Mair[14] speculated that extra sulfur can be incorporated into the organic compounds from sedimentary rocks due to the limited amount of sulfur compounds in biomass. Hanson[15] proposed that the sulfur-containing compounds may be formed during the thermal reaction between elemental sulfur and sedimentary organic matter. Some literature suggested that the reaction

Received: October 6, 2022
Revised: November 28, 2022
Accepted: January 3, 2023

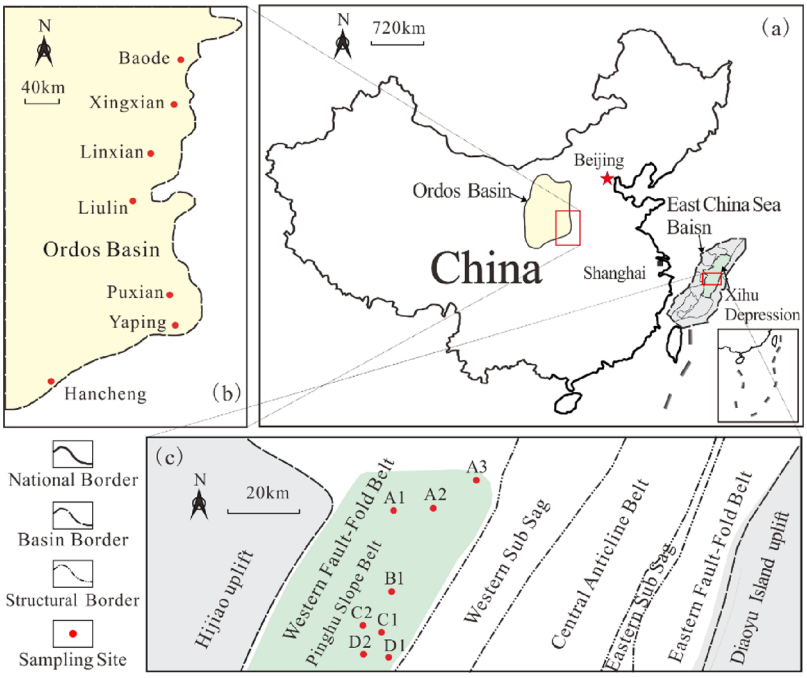

Figure 1. Map showing well locations and sampling sites of coals in the Xihu Depression and the Ordos Basin.

Table 1. Geochemical Characteristics of the Coals from the Xihu Depression and the Ordos Basin[a]

basin	sampling site	sample name	formation	type	TOC (%)	Tmax (°C)	Ro (%)	HI (mg HC/g TOC)	$S_1 + S_2$ (mg/g)	EOM (mg/g C_{org})
East China Sea Basin	Xihu Depression	A1-1	E_2p	core	39.0	428	0.64	288	118.4	103.6
		A1-2	E_2p	cuttings	45.3	437	0.74	195	93.7	35.0
		A1-3	E_2p	cuttings	58.6	457	0.88	192	124.2	16.9
		A2-1	E_2p	cuttings	65.0	460	0.96	193	140.2	11.5
		A3-1	E_2p	cuttings	37.1	461	1.00	120	50.1	52.8
		B1-1	E_2p	cuttings	62.6	427	0.63	232	150.3	50.1
		B1-2	E_2p	cuttings	39.2	430	0.69	244	100.8	92.7
		C1-1	E_2p	core	38.1	433	0.67	366	143.3	95.0
		C1-2	E_2p	core	61.0	433	0.70	356	235.7	133.5
		C1-3	E_2p	cuttings	44.6	438	0.76	203	99.8	61.6
		C2-1	E_2p	core	56.5	421	0.60	370	217.0	107.8
		C2-2	E_2p	cuttings	57.3	429	0.62	194	130.2	120.7
		D1-1	E_2p	core	74.5	437	0.74	212	167.5	160.5
		D2-1	E_2p	cuttings	53.9	436	0.72	266	157.3	64.5
Ordos Basin	Baode	BDS24	C-P	outcrop	68.6	444	0.62	246	170.8	74.3
		BDS14	C-P	outcrop	73.9	444	0.71	235	176.1	71.8
	Linxian	LXS11	C-P	outcrop	77.9	444	0.77	239	192.4	78.2
		LXS15	C-P	outcrop	91.5	463	0.96	176	166.3	11.1
		LXS8	C-P	outcrop	71.2	455	1.03	194	139.3	17.4
	Xingxian	XXS10	C-P	outcrop	74.3	440	0.73	278	209.0	69.1
	Liulin	LLS25	C-P	outcrop	84.3	493	1.40	97.4	82.7	7.8
		LLS5	C-P	outcrop	75.1	489	1.27	96.9	75.6	15.1
	Hancheng	HCS1	C-P	outcrop	80.7	498	1.66	62.9	51.7	2.7
		HCS13	C-P	outcrop	85.4	505	1.57	53.0	46.6	4.9
		HCS4	C-P	outcrop	83.8	501	1.88	48.8	41.9	4.8
	Puxian	PXS22	C-P	outcrop	83.1	435	0.62	276	243.0	137.7
		PXS6	C-P	outcrop	84.3	444	0.63	230	203.8	88.7
	Yaping	YPS9	C-P	outcrop	82.4	484	1.36	107	90.0	12.7

[a]TOC: total organic carbon; Tmax: temperature at maximum generation; Ro: vitrinite reflectance; HI: hydrogen index = $S_2 \times 100/\mathrm{TOC}$; $S_1 + S_2$: hydrocarbon generation potential; EOM: extractable organic matter.

between H_2S (hydrogen sulfide) generated by sulfate reducing bacteria with compounds in sediments can produce sulfur polycyclic compounds in the diagenesis stage.[16,17] Li et al.[3] suggested that the BNTs do not have clear biological

https://doi.org/10.1021/acsearthspacechem.2c00309
ACS Earth Space Chem. XXXX, XXX, XXX−XXX

Table 2. Absolute Concentrations of Benzonaphthothiophenes and Related Parameters of Coals from the Xihu Depression and the Ordos Basin[a]

sample name	Pr/Ph	BNTR-1	BNTR-2	[2,1]BNT/[1,2]BNT	4-MDBT/1-MDBT	BNTs (μg/g C_{org})	MDBTs (μg/g C_{org})	C_{31}22S/(22S + 22R) hopane	$C_{29}\beta\beta/(\beta\beta + \alpha\alpha)$ sterane	F_2	MPI1	%Rc (MPI1)	G/C_{30}H	DBT/P
A1-1	7.41	5.30	2.22	3.82	4.01	0.14	0.82	0.60	0.28	0.21	0.48	0.69	0.07	0.01
A1-2	7.91	2.69	1.34	2.67	1.93	2.48	1.16	0.59	0.32	0.17	0.30	0.58	0.06	0.01
A1-3	6.53	7.54	2.79	4.44	2.71	0.01	0.04	0.58	0.44	0.33	0.77	0.86	0.05	0.02
A2-1	5.69	7.86	3.47	6.22	6.14	0.05	2.14	0.57	0.51	0.30	0.52	0.71	0.02	0.05
A3-1	4.95	9.31	4.14	7.47	7.78	6.07	5.25	0.51	0.46	0.35	0.82	0.89	0.17	0.09
B1-1	7.91	3.01	1.24	2.12	1.13	1.19	0.51	0.61	0.28	0.15	0.26	0.56	0.06	0.03
B1-2	8.82	3.44	1.41	2.40	1.39	1.03	0.67	0.59	0.24	0.16	0.30	0.58	0.04	0.02
C1-1	7.87	4.11	1.81	3.25	2.01	0.19	0.41	0.61	0.22	0.14	0.25	0.55	0.07	0.04
C1-2	7.80	5.58	1.55	2.15	1.56	0.27	0.42	0.60	0.26	0.13	0.27	0.56	0.07	0.09
C1-3	6.76	5.45	2.31	4.01	2.81	9.28	1.83	0.59	0.51	0.26	0.57	0.74	0.06	0.01
C2-1	7.34	2.81	1.15	1.96	1.33	0.15	0.40	0.61	0.32	0.14	0.24	0.55	0.06	0.03
C2-2	7.80	3.33	1.83	4.07	2.82	0.92	0.64	0.59	0.34	0.19	0.39	0.64	0.05	0.02
D1-1	7.85	3.17	1.08	1.64	2.60	0.17	0.68	0.60	0.30	0.17	0.33	0.60	0.05	0.02
D2-1	8.46	2.79	1.20	2.10	2.07	0.60	0.53	0.60	0.30	0.14	0.32	0.59	0.04	0.04
BDS24	0.77	1.39	0.74	1.60	1.68	0.34	0.26	0.58	0.35	0.25	0.68	0.81	0.03	0.06
BDS14	0.99	1.37	0.74	1.63	1.67	0.37	0.34	0.59	0.31	0.26	0.65	0.79	0.03	0.06
LXS11	1.41	3.98	1.98	3.93	5.87	4.36	4.08	0.62	0.47	0.28	0.58	0.75	0.07	0.11
LXS15	1.47	7.05	3.27	6.10	4.02	0.86	0.95	0.59	0.43	0.31	0.74	0.84	0.08	0.08
LXS8	0.96	6.53	3.32	6.74	5.13	0.68	0.68	0.58	0.50	0.31	0.71	0.83	0.10	0.05
XXS10	2.00	1.42	0.81	1.88	1.72	0.85	0.35	0.60	0.36	0.27	0.65	0.79	0.03	0.02
LLS25	1.20	18.6	7.78	13.4	39.2	0.94	1.97	0.56	0.41	0.44	1.66	1.40	0.14	0.06
LLS5	1.14	15.0	6.64	11.9	29.1	0.36	0.40	0.56	0.57	0.44	1.37	1.22	0.20	0.06
HCS1	0.77	19.7	8.14	13.9	45.7	1.39	1.51	0.61	0.45	0.53	1.25	1.15	0.15	0.09
HCS13	0.49	18.8	7.74	13.2	47.3	2.32	2.76	0.59	0.48	0.51	1.22	1.13	0.19	0.10
HCS4	0.70	21.5	9.23	16.2	55.1	0.67	0.98	0.53	0.45	0.52	1.40	1.24	0.20	0.09
PXS22	1.40	2.14	1.18	2.65	1.87	0.59	0.40	0.59	0.48	0.26	0.68	0.81	0.04	0.03
PXS6	1.10	3.02	1.68	3.78	2.09	0.60	0.45	0.59	0.50	0.26	0.65	0.79	0.05	0.03
YPS9	0.73	16.3	6.69	11.4	31.1	2.39	1.05	0.53	0.41	0.43	1.39	1.23	0.22	0.06

[a]Pr/Ph: pristane/phytane; BNTR-1: benzo[*b*]naphtho[2,1-*d*]thiophene/benzo[*b*]naphtho[2,3-*d*]thiophene; BNTR-2: benzo[*b*]naphtho[2,1-*d*]thiophene/(benzo[*b*]naphtho[1,2-*d*]thiophene+benzo[*b*]naphtho[2,3-*d*]thiophene); [2,1]BNT/[1,2]BNT: benzo[*b*]naphtho[2,1-*d*]thiophene/benzo[*b*]naphtho[1,2-*d*]thiophene; 4-MDBT/1-MDBT: 4-methyldibenzothiophene/1-methyldibenzothiophene; BNTs: sum of the absolute concentrations of benzo[*b*]naphtho[2,1-*d*]thiophene, benzo[*b*]naphtho[1,2-*d*]thiophene, and benzo[*b*]naphtho[2,3-*d*]thiophene; MDBTs: sum of the absolute concentrations of 1-, 2-, 3-, and 4-methyldibenzothiophene; F_2: 2-MP/(1-MP + 2-MP + 3-MP + 9-MP); MPI1: 1.5 × (2-MP + 3-MP)/(P + 1-MP + 9-MP); %Rc (MPI1): calculated vitrinite reflectance by MPI1; G/C_{30}H: gammacerane/C_{30} hopane; DBT/P: dibenzothiophene/phenanthrene.

https://doi.org/10.1021/acsearthspacechem.2c00309
ACS Earth Space Chem. XXXX, XXX, XXX−XXX

precursors. Based on laboratory experiments, Kropp et al.[18] suggested that *Pseudomonas* can produce the BNTs from benzo[*b*]thiophenes. However, less work has been done on the formation mechanism of BNTs in coals.

Some work has been accomplished on the geochemical significance of BNTs. Li et al.[7] proposed that absolute concentrations of BNTs and benzo[*b*]naphtho[2,1-*d*]-thiophene/(benzo[*b*]naphtho[2,1-*d*]thiophene + benzo[*b*]-naphtho[1,2-*d*]thiophene) ([2,1]BNT/([2,1]BNT + [1,2]BNT)) can trace the oil migration distance. Fang et al.[6] successfully employed [2,1]BNT/([2,1]BNT + [1,2]BNT) to track the migration orientations and filling pathways of oils in carbonate reservoirs from the Tarim Basin. Yang et al.[11] also used the same parameter to trace oil migration orientations of condensates and light oils into lacustrine clastic reservoirs of the Beibuwan Basin. Panda et al.[19] proposed a migration indicator, namely, the BNT ratio ([2,1]BNT/[1,2]BNT), and used it to track oil migration in Saudi Arabian fields. Subsequently, the BNT ratio was successfully applied in mapping migration pathways and constructing filling sequences of oil fields, in comparison with benzocarbazoles.[5,8] However, the effect of thermal maturity on the distributions of BNTs is not clear, which may cause some problems in the applicability of BNTs to track migration pathways if the thermal history is not well constrained and when dealing with samples of variable thermal maturities.

In this paper, three BNT isomers were firmly identified in coals by comparison with the retention indices reported in the literature. The thermodynamic stabilities of BNT isomers were determined by density functional theory (DFT) calculations. We described the distribution patterns of BNTs in coals from the Xihu Depression (East China Sea Basin) and the Ordos Basin in China. The effects of thermal maturity on the distributions of BNTs and their geochemical application are discussed.

2. GEOLOGIC SETTING AND SAMPLES

The East China Sea Basin, at the edge of the eastern China, is the largest petroliferous basin in offshore China (Figure 1a). It is a Mesozoic−Cenozoic back-arc rift basin created by upwelling of the back-arc deep material and asthenosphere rise.[20−22] The Xihu Depression, located in the northeast of the East China Sea Basin, is an important hydrocarbon-producing depression with an area of approximately 5.9×10^4 km^2 (Figure 1c). Previous studies have basically agreed that the Pinghu Formation (E_2p) coal measures are the primary source rocks.[23−26] The source rocks in the Pinghu Formation are composed of mudstones, carbonaceous mudstones, and coals.[24,27] The E_2p was mainly developed in a lacustrine-swamp depositional environment.[26,28] Fourteen coals were collected from the Pinghu Formation in the Xihu Depression. The total organic carbon (TOC) content ranges from 37.1 to 74.5% (Table 1). The hydrocarbon generation potential (S_1 + S_2) varies from 50.1 to 235.7 mg/g. The hydrogen index (HI) is in the range of 120−370 mg HC/g TOC, corresponding to type II−III kerogen based on the hydrogen index versus Tmax (°C) plot. Rock-Eval Tmax is widely used to assess thermal maturity, although it is known to be affected by many factors.[29] The coals studied in this study have vitrinite reflectance (%Ro) values of 0.60−1.00 %Ro and have Tmax values of 421−461 °C, indicating that the samples are low mature to mature (Table 1). The pristane/phytane (Pr/Ph) values of the coals are high with a range of 4.95−8.82, consistent with their depositional environments and relatively low thermal maturities (Table 2).

The Ordos Basin is located in North-Central China with an area of 37×10^4 km^2 and is the second largest sedimentary basin in China. Many large gas fields have been discovered in the upper Paleozoic strata (Figure 1b).[30−32] The consensus has been reached that the natural gases in the upper Paleozoic reservoirs originate from Carboniferous−Permian coal measure source rocks.[33−35] The sedimentary environment of Carboniferous−Permian source rocks were marine−terrestrial transitional facies, and their lithology are mainly coals, mudstones, and carbonaceous mudstones.[36] Fourteen coal samples from this basin were sampled in the Carboniferous−Permian formations. The TOC content and hydrocarbon generation potential (S_1 + S_2) of the coals exhibit a wide range of values, from 68.6 to 91.5% and 41.9 to 243.0 mg/g, respectively. Hydrocarbon index (HI) values of the coal samples are in the range of 48.8−277 mg HC/g TOC (Table 1). The plot of HI vs Tmax shows that most of the coal samples are type II−III kerogen. Tmax and vitrinite reflectance values of the coal samples are in the range of 435−505 °C and 0.62−1.88 %Ro, respectively (Table 1). The coal samples have low Pr/Ph values of 0.49−2.00 (Table 2).

3. METHODS

3.1. Experimental Methods. The coal samples were crushed to <80 mesh (0.2 mm) in diameter. Rock-Eval pyrolysis was carried out on the OGE pyrolysis apparatus, yielding results similar to the traditional Rock-Eval pyrolysis analyzer.[37,38] Before analysis, contaminants and carbonates were removed from the coals by deionized water and hydrochloric acid, respectively. Then, the LECO CS-230 carbon/sulfur analyzer was used to obtain TOC content. The vitrinite reflectance values of coals were measured on a Leica Model MPV-SP microscopic photometer on the basis of the method of Kilby.[39]

To extract soluble organic matter, the powder coals were processed for 48 h in a Soxhlet apparatus using 400 mL of dichloromethane/methanol (93:7, v:v). Asphaltenes were removed from the extracts by precipitation using petroleum ether and then fractionated into saturated, aromatic, and resin fractions by liquid chromatography using alumina/silica gel column. The elution solvents used were, respectively, petroleum ether, dichloromethane:petroleum ether (2:1, v:v), and dichloromethane:methanol (93,7, v:v). The analyses of aromatic fractions were carried out on an Agilent 6890 gas chromatography coupled to 5975i MS equipped with a HP-5MS column (60 m × 0.25 mm i.d., 0.25 μm film thickness). The gas chromatography−mass spectrometry (GC−MS) operating conditions were as follows: initial temperature was kept at 80 °C for 1 min, then raised to 310 °C at 3 °C/min, and finally held isothermal for 16 min. Helium was the carrier gas, and the temperature of injector was set at 300 °C. The mass spectrometry was used in electron impact (EI) mode with ionization energy of 70 eV and a scan range of 50−600 Da.

3.2. Quantification of Aromatic Compounds. Prior to GC−MS analysis, a known amount of perdeuterated phenanthrene (phenanthrene-d_{10}) was added to the aromatic hydrocarbon fraction samples, which was identified in m/z 188 mass chromatogram. The peak area of methyldibenzothiophenes (MDBTs) and BNTs can be determined on the m/z 198 and m/z 234 mass chromatograms, respectively.

https://doi.org/10.1021/acsearthspacechem.2c00309
ACS Earth Space Chem. XXXX, XXX, XXX−XXX

4. RESULTS AND DISCUSSION

4.1. Identification of Benzonaphthothiophenes. Benzonaphthothiophenes have been detected in coal liquids, shale oils, shales, marine carbonates, and oils.[2,3,5,6,11,12] The occurrence of benzonaphthothiophenes in coals have been rarely detected. In this study, benzonaphthothiophenes were unequivocally identified in coals by comparison with retention indices reported in previous studies. In order to compare the retention behaviors of compounds on different chromatographic columns, the retention index system has been used.[40,41] The retention index (I) markers for temperature-programmed GC conditions for polycyclic aromatic compounds are a series of aromatic hydrocarbons with different ring numbers, which are benzene (I = 100), naphthalene (I = 200), phenanthrene (I = 300), and chrysene (I = 400).[10,37,38,42] According to the equation proposed by Vassilaros et al.,[10] we accurately calculated the retention indices of benzonaphthothiophenes. The elution order of the benzonaphthothiophenes is determined as follows: [2,1]BNT, [1,2]BNT, [2,3]BNT (Figure 2), which is in agreement with

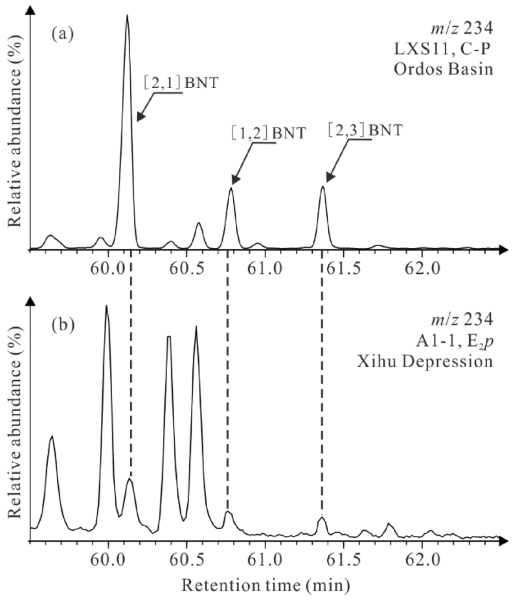

Figure 2. Identification of benzonaphthothiophene isomers in mass chromatograms (m/z 234) in the coals.

previous studies.[3,6,9,10] Retention indices for these three benzonaphthothiophene isomers on the HP-5MS column in the present study show good agreement with those reported in the literature (Table 3).[3,9,10] Therefore, benzonaphthothiophenes were firmly assigned in the coals.

4.2. Thermodynamics of Benzonaphthothiophenes. At present, density functional theory (DFT) calculation has become a powerful tool to gain better insight into the molecular level phenomena in geochemistry.[38,43−45] All the DFT calculations of thermodynamic properties, such as Gibbs free energy (ΔG), internal energy (ΔU), electron energy (ΔE), and enthalpy (ΔH) were conducted by using the Gaussian 09 program.[38,43] The molecular structures were fully optimized at the B3LYP/6-311++G (d,p) level of theory.[38,43]

The calculation of thermodynamic properties for BNT isomers indicates that [2,1]BNT is the most stable isomer with the lowest energy, followed by [2,3]BNT. The [1,2]BNT has the highest energy and signifies the least thermodynamic stability (Table 4). Thus, the thermodynamic stability of

Table 4. Thermodynamic Properties of Benzonaphthothiophenes[a]

isomer	ΔE (kcal/mol)	ΔU (kcal/mol)	ΔH (kcal/mol)	ΔG (kcal/mol)
[2,1]BNT	0.00	0.00	0.00	0.00
[2,3]BNT	2.01	2.00	2.00	2.00
[1,2]BNT	3.49	3.57	3.57	2.79

[a][2,1]BNT: benzo[b]naphtho[2,1-d]thiophene; [2,3]BNT: benzo[b]naphtho[2,3-d]thiophene; [1,2]BNT: benzo[b]naphtho[1,2-d]thiophene.

benzonaphthothiophenes follows the following order: [2,1]BNT > [2,3]BNT > [1,2]BNT (Table 4). The previous literature reported that the differences in the thermodynamic stabilities and Gibbs free energies for individual isomers of polycyclic aromatic compounds are mainly the result of steric hindrance.[38,43,46] Steric hindrance causes thermodynamic instability due to the presence of the naphthalene and benzene rings at the thiophene ring with different substitution positions (Figure 3). With regard to [1,2]BNT, these angles between the naphthalene ring, benzene ring, and thiophene ring are severely deformed from the ideal 120° (Figure 3a). This causes the increase of total energy and makes it unstable. However, for [2,1]BNT and [2,3]BNT, these corresponding angles are less deformed, resulting in the decrease of total energy and instability. Significantly, the lone paired electrons of the sulfur atom are able to form a hydrogen bond with the hydrogen atom of the naphthalene ring at C-1, which makes it the most stable isomer. The bond length of H···S is 2.830 Å, which is within the range of the hydrogen bond. Li et al.[47] suggested that the hydrogen bond (2.970 Å) between the oxygen atom in 4-methyldibenzofuran and the hydrogen atoms of methyl can readily form.

4.3. Effects of Maturity on Distribution Patterns of Benzonaphthothiophenes. In this paper, benzonaphtho-

Table 3. Retention Indices of Benzonaphthothiophenes[a]

compounds	reference (HP-5MS)[3]		coal, Ordos Basin (HP-5MS)		coal, Xihu Depression (HP-5MS)		identification
	t_R	I	t_R	I	t_R	I	
phenanthrene	41.874	300.00	41.660	300.00	41.597	300.00	phenanthrene
benzo[b]naphtho[2,1-d]thiophene	60.431	389.91	60.199	389.59	60.132	389.52	benzo[b]naphtho[2,1-d]thiophene
benzo[b]naphtho[1,2-d]thiophene	61.045	392.89	60.859	392.78	60.816	392.83	benzo[b]naphtho[1,2-d]thiophene
benzo[b]naphtho[2,3-d]thiophene	61.638	395.76	61.445	395.61	61.405	395.67	benzo[b]naphtho[2,3-d]thiophene
chrysene	62.517	400.00	62.353	400.00	62.298	400.00	chrysene

[a]t_R:retention time; I: retention index. Retention indices of benzonaphthothiophenes according to Li et al.[3]

https://doi.org/10.1021/acsearthspacechem.2c00309
ACS Earth Space Chem. XXXX, XXX, XXX−XXX

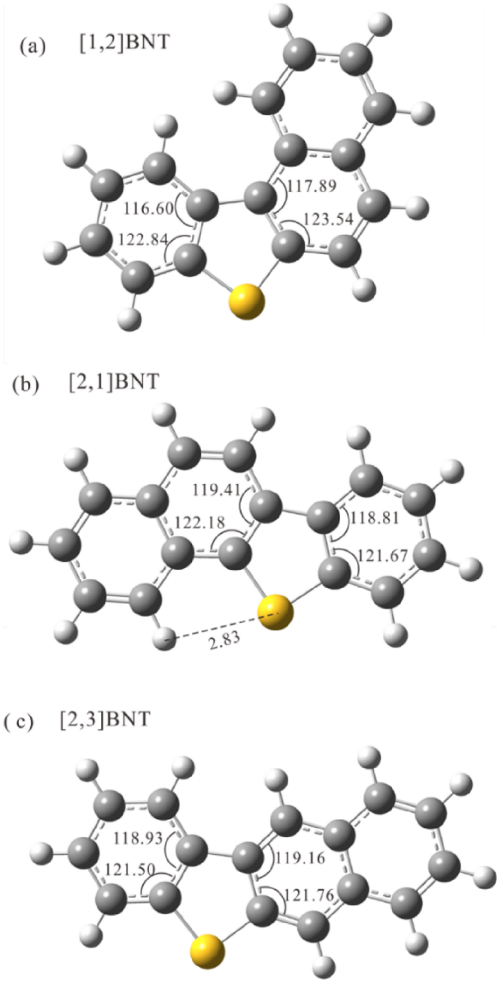

Figure 3. Optimized geometries of (a) [1,2]BNT, (b) [2,1]BNT, and (c) [2,3]BNT.

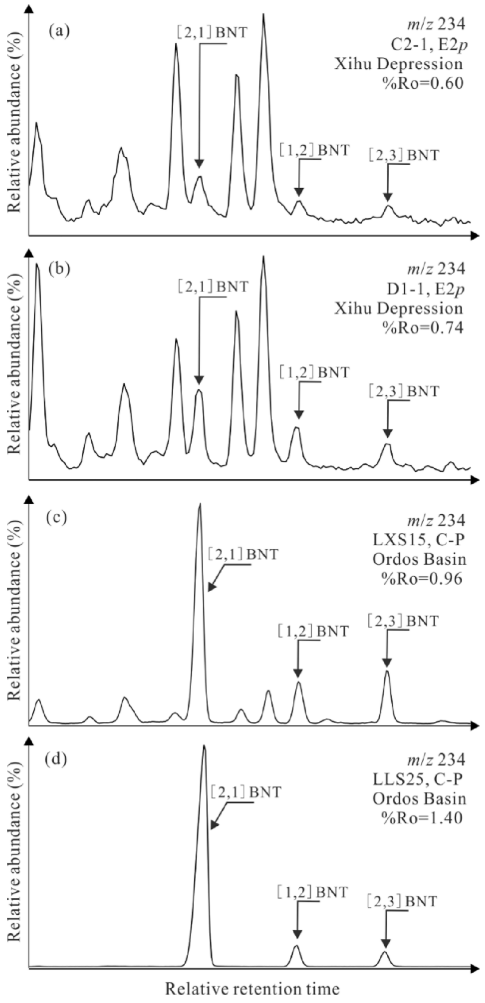

Figure 4. Effects of thermal maturity on the distributions of benzonaphthothiophenes for the coals.

thiophenes were identified in the coals from the Xihu Depression and the Ordos Basin. Figure 4 illustrates the distribution characteristics of the benzonaphthothiophenes in coal samples with various thermal maturities. For coals at low levels of thermal stress (≤0.7%Ro), the contents of [1,2]BNT, [2,1]BNT and [2,3]BNT are all low (Figure 4a). Interestingly, the more mature (= 0.7−1.4%Ro) coals contain [2,1]BNT as the dominant compound, while [1,2]BNT and [2,3]BNT occur in low abundance (Figure 4b,c), which is consistent with the results of previous studies.[48−50] Furthermore, for coals with high thermal maturities (>1.4%Ro), the abundance of [2,1]BNT is high and significantly higher than that of [1,2]BNT and [2,3]BNT (Figure 4d). Coincidentally, the distribution characteristics of BNTs in the highly mature shales with %Ro > 1.4 are similar to that in the coals with high thermal maturities.[12] Obviously, compared with [2,1]BNT, the relative amounts of [2,3]BNT and [1,2]BNT show overall decreases with the increase of thermal maturity. On the basis of the distribution characteristics of BNTs in the coals, the concentration of [2,1]BNT relative to [2,3]BNT and [1,2]BNT is obviously affected by thermal maturity. We can reasonably suggest that thermodynamic stability of [2,1]BNT is higher than that of [2,3]BNT and [1,2]BNT, which is in agreement with the stability order calculated by DFT.

According to theoretical calculations and geochemical data, we propose two thermal maturity parameters of BNTs in this study, which are BNTR-1 ([2,1]BNT/[2,3]BNT) and BNTR-2 ([2,1]BNT/([1,2]BNT + [2,3]BNT)). Figure 5 shows that BNTR-1 and BNTR-2 values both exhibit overall increases with increasing thermal maturity. For the coals with %Ro = 0.6−0.8, BNTR-1 and BNTR-2 both keep low values, which are nearly constant. Interestingly, BNTR-1 and BNTR-2 values obviously increase with the increasing thermal maturity at high thermal maturities with %Ro > 0.9. Previous studies proposed the distribution patterns of polycyclic aromatic compounds are thermodynamically controlled at high thermal maturity and kinetically controlled at low thermal maturity.[51,52] The increases of BNTR-1 and BNTR-2 values suggested an increase in the content of the more stable isomer ([2,1]BNT) and decreases in the contents of less stable isomers ([1,2]BNT and [2,3]BNT) after the oil generation peak (>0.9%Ro). This can be attributed to the formation mechanism of BNTs. The less stable isomers ([1,2]BNT and [2,3]BNT) due to their lower initial formation enthalpy are ready to be formed at low maturity.[38,43,53] With increasing thermal maturity, the less stable isomers ([1,2]BNT and [2,3]BNT) may be degraded or probably transform into other more condensed compounds. Thus, the abundance of [2,1]BNT relative to [1,2]BNT and [2,3]BNT displays an overall increase with increasing thermal maturity. Figure 5 shows that BNTR-1 and BNTR-2 have good linear relation-

https://doi.org/10.1021/acsearthspacechem.2c00309
ACS Earth Space Chem. XXXX, XXX, XXX−XXX

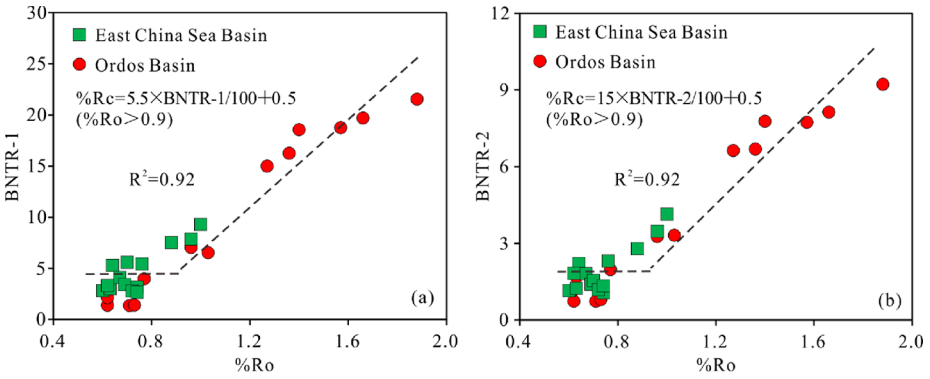

Figure 5. Cross plots showing correlations between vitrinite reflectance (%Ro) vs (a) BNTR-1, (b) BNTR-2 of the coals.

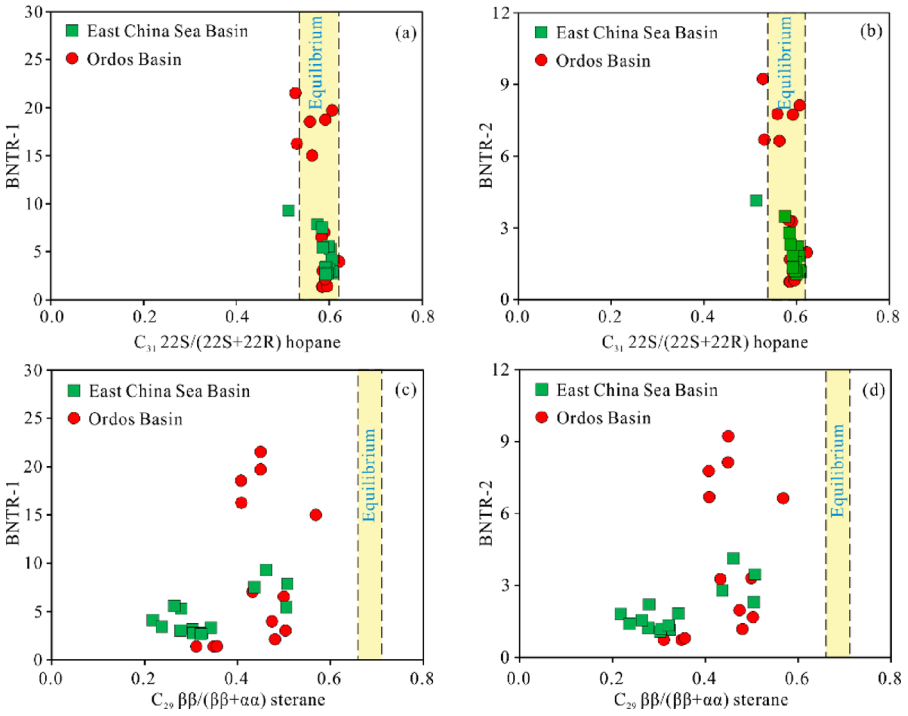

Figure 6. Cross plots showing correlations of C_{31} 22S/(22S + 22R) hopane and C_{29} $\beta\beta/(\beta\beta + \alpha\alpha)$ sterane vs BNTR-1 and BNTR-2 of the coals.

ships with the measured vitrinite reflectance (%Ro = 0.96−1.88). We preliminarily established the calibrations of BNTR-1 and BNTR-2 against %Ro, and the specific relationships are: %Rc = 5.5 × BNTR-1/100 + 0.5 (%Ro > 0.9) and %Rc = 15 × BNTR-2/100 + 0.5 (%Ro > 0.9) with related coefficients (R^2) up to 0.92. This indicates that BNTR-1 and BNTR-2 are good maturity indicators at high levels of thermal stress.

4.4. Correlations between BNTR-1, BNTR-2, and Other Maturity Indicators. The C_{31} 22S/(22S + 22R) hopane is useful as a thermal maturity parameter for immature to low mature range, where values ranging from 0.57 to 0.62 indicate that the oil window has been reached.[54,55] Seifert and Moldowan[56] proposed C_{29} $\beta\beta/(\beta\beta + \alpha\alpha)$ sterane as a valid maturity parameter for immature to mature range, which achieves equilibrium at 0.67−0.71. As we can see from Figure 6a,b, BNTR-1 and BNTR-2 ratios increase with increasing thermal maturity and even C_{31} 22S/(22S + 22R) hopane values achieve the equilibrium (0.57−0.62). The BNTR-1 and BNTR-2 ratios keep nearly low constant values at C_{29} $\beta\beta/(\beta\beta + \alpha\alpha)$ sterane = 0.22−0.36. BNTR-1 and BNTR-2 ratios show an increase with C_{29} $\beta\beta/(\beta\beta + \alpha\alpha)$ sterane = 0.41−0.57 (Figure 6c,d). Interestingly, for the coals with vitrinite reflectance > 1.0%Ro, the C_{29} $\beta\beta/(\beta\beta + \alpha\alpha)$ sterane ratios are in the range of 0.41−0.57, which do not reach the equilibrium (0.67−0.71). Peters et al.[57] suggested that high thermal maturity may cause the C_{29} $\beta\beta/(\beta\beta + \alpha\alpha)$ sterane values to decrease, which may be the reason for the phenomenon observed here. The change trend is similar to the variation tendency of BNTR-1 and BNTR-2 values with increasing %Ro values. Compared with the C_{31} 22S/(22S + 22R) hopane and the C_{29} $\beta\beta/(\beta\beta + \alpha\alpha)$ sterane ratios, the BNTR-1 and BNTR-2 have a wider range of application as a thermal maturity indicator.

Kvalheim et al.[58] proposed that the methylphenanthrene (MP) distribution fraction (F_2 = 2-MP/(1-MP + 2-MP + 3-MP + 9-MP)) can be a useful maturity indicator. The methylphenanthrene index (MPI1) was a widely used maturity parameter for organic matter, and the calculated vitrinite reflectance (%Rc (MPI1)) can be determined according to the equation proposed by Radke.[59] As can be seen from Figure 7, BNTR-1 and BNTR-2 values both show an overall increase with the increase of F_2, MPI1, and %Rc (MPI1) values, which

https://doi.org/10.1021/acsearthspacechem.2c00309
ACS Earth Space Chem. XXXX, XXX, XXX−XXX

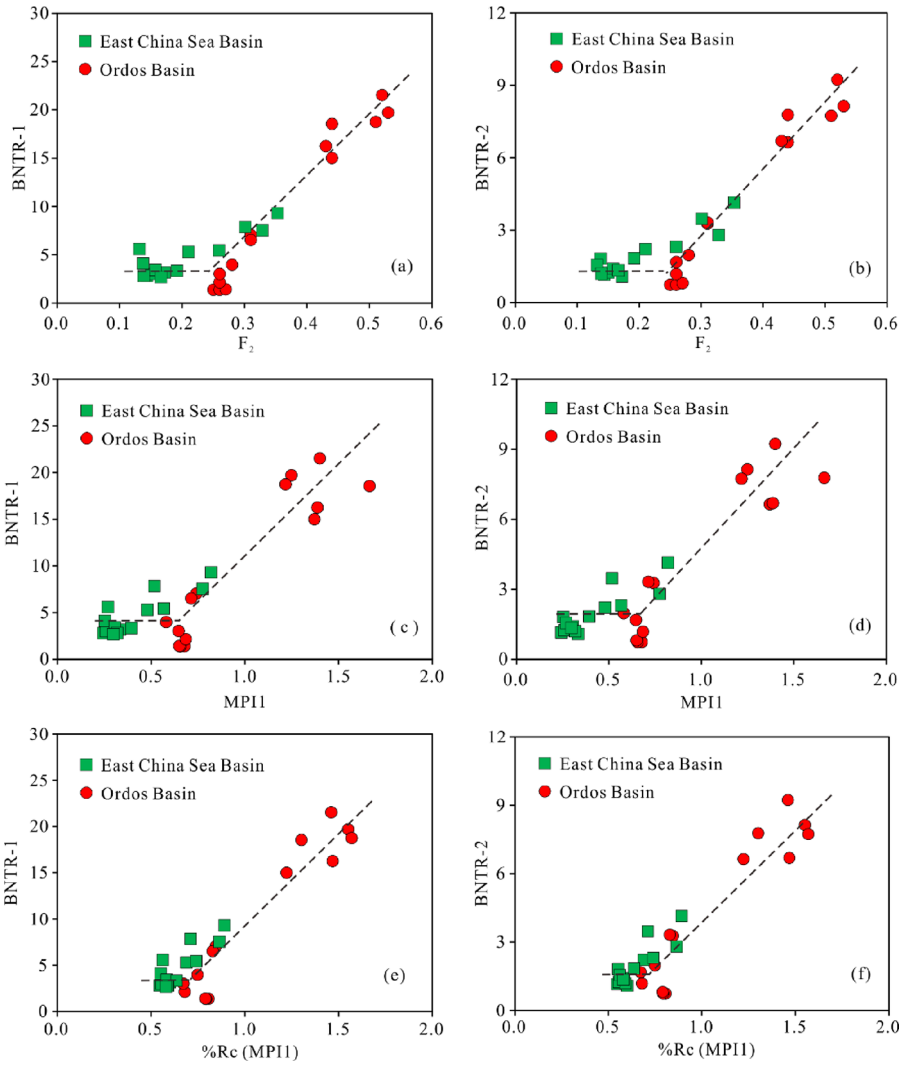

Figure 7. Cross plots showing correlations of F_2, MPI1, and %Rc (MPI1) vs BNTR-1 and BNTR-2 of the coals.

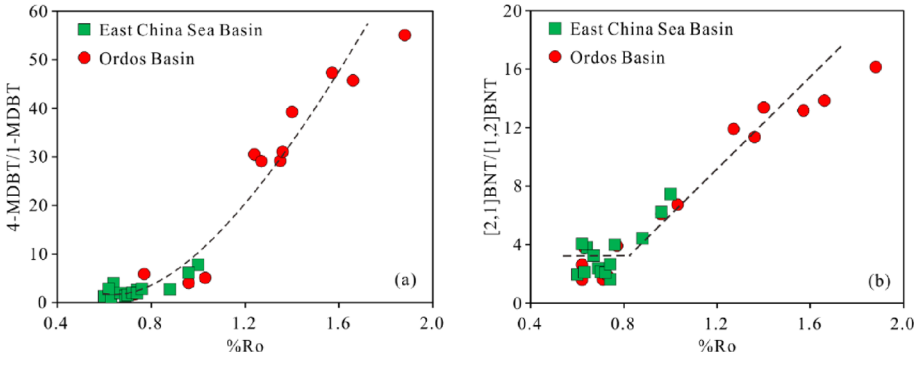

Figure 8. Cross plots showing correlations of vitrinite reflectance (%Ro) vs (a) 4-MDBT/1-MDBT and (b) [2,1]BNT/[1,2]BNT of the coals.

contain two parts. The BNTR-1 and BNTR-2 values keep nearly low constant values at F_2 = 0.13−0.28, MPI1 = 0.24−0.68, and %Rc (MPI1) = 0.54−0.89. However, BNTR-1 and BNTR-2 values then generally increase with the increase of F_2, MPI1, and %Rc (MPI1) values (F_2 > 0.3, MPI1 > 0.7, and %Rc (MPI1) > 0.9) at high maturity stage. The results are similar to the change trend of BNTR-1 and BNTR-2 values with increasing vitrinite reflectance. Thus, BNTR-1 and BNTR-2 show good relationships with the widely used thermal maturity indicators, illustrating that they are useful maturity indicators at high thermal maturity stage.

4.5. Comparison of the Distribution Patterns of Benzonaphthothiophenes and Methyldibenzothiophenes. In order to gain a better insight into the formation mechanism of the BNTs, we compared the distributions of the BNTs and methyldibenzothiophenes (MDBTs). The methyldibenzothiophene ratio (MDR = 4-MDBT/1-MDBT) has been widely used as an effective indicator of maturity.[7,60−62]

https://doi.org/10.1021/acsearthspacechem.2c00309
ACS Earth Space Chem. XXXX, XXX, XXX−XXX

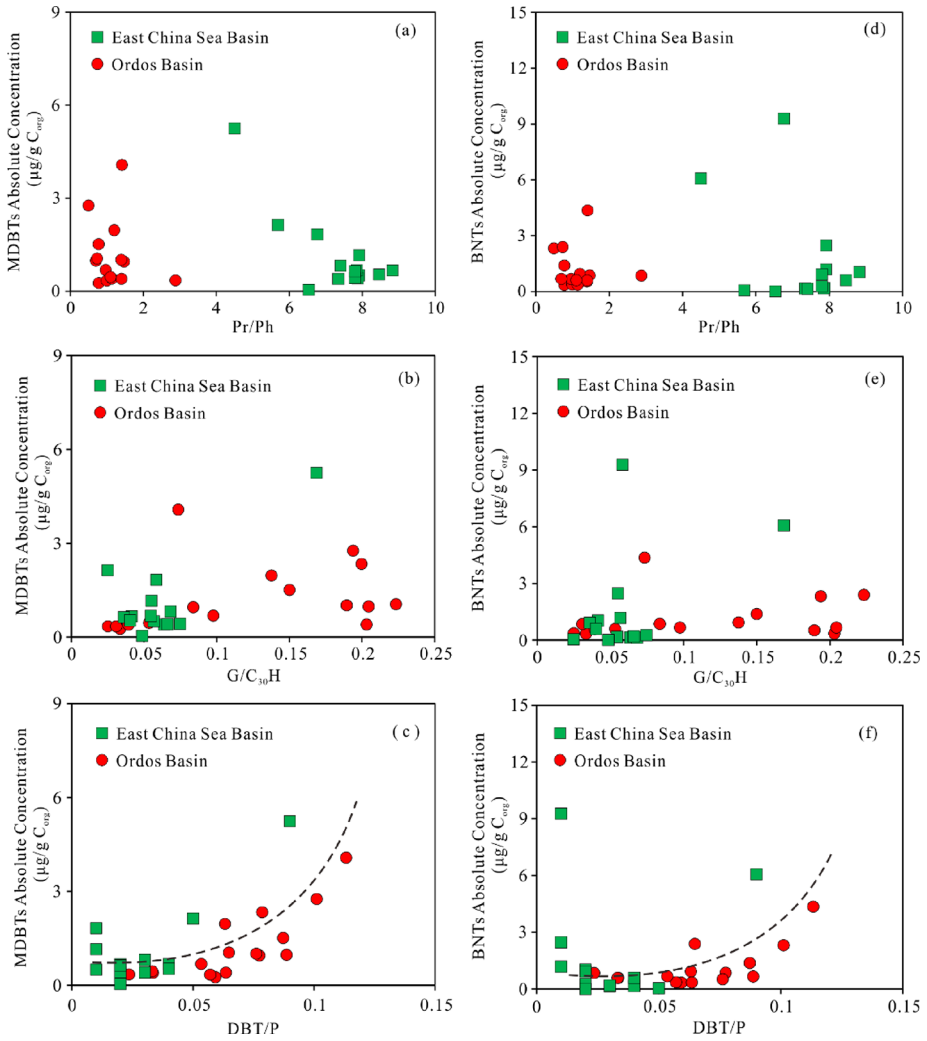

Figure 9. Cross plots showing correlations of Pr/Ph, $G/C_{30}H$, and DBT/P vs the absolute concentration of MDBTs and BNTs of the coals.

The BNT ratio ([2,1]BNT/[1,2]BNT) was widely used in tracking oil migration.[5,8,19] We compared the [2,1]BNT/[1,2]BNT and 4-MDBT/1-MDBT ratios with the increasing vitrinite reflectance. The 4-MDBT/1-MDBT values gradually increase with the increase of vitrinite reflectance with %Ro > 0.6, which is consistent with the phenomenon reported by the previous literature.[7,62,63] However, the 1-MDBT concentration in high mature coals with %Ro > 1.2 are very low, resulting in the MDR values of >30 (Figure 8a). Therefore, we should be cautious about the accuracy of the MDR ratio when it is applied to estimate the maturity at high thermal stress.[63] However, the concentrations of [2,1]BNT, [1,2]BNT, and [2,3]BNT are comparable in the highly mature coals, resulting in BNTR-1 and BNTR-2 values of 15.0−21.5 and 6.64−9.23, respectively. Therefore, the BNTR-1 and BNTR-2 may be more suitable for maturity evaluation during high thermal maturity stage. Significantly, [2,1]BNT/[1,2]BNT values keep nearly low constant values with %Ro < 0.9 and then show a gradual increase with increasing vitrinite reflectance after %Ro = 0.9 (Figure 8b). Li et al.[7] reported that the thermal maturity does not alter the BNT migration ratio for oils generated within the main oil window, which agrees with the phenomenon of this study. Similarly, Arouri and Panda[5] suggested that the variations in BNTs were ascribed to migration fractionation in an oil system of low thermal maturity (0.78−0.84 %Ro). This result shows that thermal maturity has little effect on the BNT ratio at low thermal maturity, and this parameter is suitable for tracking oil migration during the main oil generating window. However, thermal maturity can have marked effects on the BNT ratio at high maturity stage. Therefore, we should be cautious in applying this parameter in tracing oil migration in fluids of higher maturities.

In this study, in order to compare the differences between benzonaphthothiophenes and methyldibenzothiophenes, the BNT and MDBT absolute concentrations, pristane/phytane ratio (Pr/Ph), gammacerane/C_{30} hopane ($G/C_{30}H$), and dibenzothiophene/phenanthrene (DBT/P) were investigated (Table 2). The Pr/Ph is an effective indicator for redox conditions in the deposition process.[54,64] The high $G/C_{30}H$ ratio can often be traced to hypersaline depositional environments.[65] The DBT/P can be used to assess the availability of reduced sulfur for incorporation into organic matter during deposition.[66] The sedimentary environment with a higher DBT/P ratio generally has higher total sulfur content.[66] No clear trend for the absolute concentrations of MDBTs with increasing Pr/Ph and $G/C_{30}H$ ratios was found (Figure 9a,b). Previous studies suggested that an anoxic environment contributes to the generation of MDBTs,[67,68] which is not consistent with the result observed in this paper. The salinity of

https://doi.org/10.1021/acsearthspacechem.2c00309
ACS Earth Space Chem. XXXX, XXX, XXX−XXX

the water during deposition has little influence on the formation of MDBTs. Similarly, with the increase of Pr/Ph and G/C_{30}H values, the absolute BNT concentrations also show no obvious regular change trend (Figure 9d,e). These results suggest that redox conditions and water salinity during deposition may not be the significant controlling factor for the variations observed in the BNTs. However, the absolute concentrations of MDBTs and BNTs both display an overall increase with increasing DBT/P values (Figure 9c,f). This indicates that the sedimentary environment, having high availability of reduced sulfur for incorporation into organic matter or high total sulfur content, is likely more beneficial to the generation of BNTs and MDBTs. Although we did not make the formation mechanism of BNTs clear in this paper, the similarities of MDBTs and BNTs under different formation environments and their behaviors with increasing thermal maturity have been preliminarily observed.

5. CONCLUSIONS

All three benzonaphthothiophene isomers were unequivocally identified in coals by comparison with the retention indices reported in the previous literature. Judging from the thermodynamic properties, the stability of BNTs is in the following order: [2,1]BNT > [2,3]BNT > [1,2]BNT. For the coals with %Ro < 0.7, the concentrations of BNT isomers are low. The abundance of [2,1]BNT relative to [1,2]BNT and [2,3]BNT shows an overall increase with increasing thermal maturity during high maturity stage (%Ro > 0.9). According to distributions of BNTs and calculated stabilities, two maturity indicators, i.e., BNTR-1 ([2,1]BNT/[2,3]BNT) and BNTR-2 ([2,1]BNT/([1,2]BNT + [2,3]BNT)), were proposed, which are valuable for maturity assessment during high maturity stage. Two calibrations of BNTR-1 and BNTR-2 against measured vitrinite reflectance were preliminarily established, which are %Rc = 5.5 × BNTR-1/100 + 0.5 (%Ro > 0.9) and %Rc = 15 × BNTR-2/100 + 0.5 (%Ro > 0.9). BNTR-1 and BNTR-2 have good correlations with the widely used molecular maturity parameters. Caution should be exercised when the [2,1]BNT/[1,2]BNT ratio is applied to trace the migration of oil during high maturity stage. The redox conditions and water salinity during deposition have little effect on the formation of BNTs. This study broadens the current understanding of the occurrence and distributions of benzonaphthothiophenes in sedimentary organic matter.

AUTHOR INFORMATION

Corresponding Author

Zhihuan Zhang − *State Key Laboratory of Petroleum Resources and Prospecting, China University of Petroleum (Beijing), Beijing 102249, China; College of Geosciences, China University of Petroleum (Beijing), Beijing 102249, China;* orcid.org/0000-0001-9224-3365; Email: zhangzh3996@vip.163.com

Author

Jiayang Li − *State Key Laboratory of Petroleum Resources and Prospecting, China University of Petroleum (Beijing), Beijing 102249, China; College of Geosciences, China University of Petroleum (Beijing), Beijing 102249, China*

Complete contact information is available at: https://pubs.acs.org/10.1021/acsearthspacechem.2c00309

Notes

The authors declare no competing financial interest.

ACKNOWLEDGMENTS

The authors are grateful to SINOPEC Shanghai Offshore Oil & Gas Company for supplying the samples. The authors would like to extend our appreciation to the editor Dr. Julie Granger and the anonymous reviewers for their constructive suggestions and comments, which improved the final paper.

REFERENCES

(1) Borwitzky, H.; Schomburg, G. Separation and identification of polynuclear aromatic compounds in coal tar by using glass capillary chromatography including combined gas chromatography-mass spectrometry. *J. Chromatogr. A* **1979**, *170*, 99−124.

(2) Willey, C.; Iwao, M.; Castle, R. N.; Lee, M. L. Determination of sulfur heterocycles in coal liquids and shale oils. *Anal. Chem.* **1981**, *53*, 400−407.

(3) Li, M.; Wang, T. G.; Simoneit, B. R. T.; Shi, S.; Zhang, L.; Yang, F. Qualitative and quantitative analysis of dibenzothiophene, its methylated homologues, and benzonaphthothiophenes in crude oils, coal, and sediment extracts. *J. Chromatogr. A* **2012**, *1233*, 126−136.

(4) Vuković, N.; Životić, D.; Mendonça Filho, J. G.; Kravić-Stevović, T.; Hámor-Vidó, M.; de Oliveira Mendonça, J.; Stojanović, K. The assessment of maturation changes of humic coal organic matter−Insights from closed-system pyrolysis experiments. *Int. J. Coal Geol.* **2016**, *155*, 213−239.

(5) Arouri, K. R.; Panda, S. K. Benzonaphthothiophene migration tracer: Selective separation and comparison with nitrogen tracers. *Mar. Pet. Geol.* **2022**, *135*, No. 105388.

(6) Fang, R.; Wang, T. G.; Li, M.; Xiao, Z.; Zhang, B.; Huang, S.; Shi, S.; Wang, D.; Deng, W. Dibenzothiophenes and benzo[*b*]-naphthothiophenes: Molecular markers for tracing oil filling pathways in the carbonate reservoir of the Tarim Basin, NW China. *Org. Geochem.* **2016**, *91*, 68−80.

(7) Li, M.; Wang, T.-G.; Shi, S.; Liu, K.; Ellis, G. S. Benzo[*b*]-naphthothiophenes and alkyl dibenzothiophenes: Molecular tracers for oil migration distances. *Mar. Pet. Geol.* **2014**, *57*, 403−417.

(8) Yang, Y.; Arouri, K. A simple geotracer compositional correlation analysis reveals oil charge and migration pathways. *Sci. Rep.* **2016**, *6*, 23066.

(9) Mössner, S. G.; Lopez De Alda, M. J.; Sander, L. C.; Lee, M. L.; Wise, S. A. Gas chromatographic retention behavior of polycyclic aromatic sulfur heterocyclic compounds, (dibenzothiophene, naphtho[*b*]thiophenes, benzo[*b*]naphthothiophenes and alkyl-substituted derivatives) on stationary phases of different selectivity. *J. Chromatogr. A* **1999**, *841*, 207−228.

(10) Vassilaros, D. L.; Kong, R. C.; Later, D. W.; Lee, M. L. Linear retention index system for polycyclic aromatic compounds: Critical evaluation and additional indices. *J. Chromatogr. A* **1982**, *252*, 1−20.

(11) Yang, L.; Li, M.; Wang, T.-G.; Shi, Y. Dibenzothiophenes and benzonaphthothiophenes in oils, and their application in identifying oil filling pathways in Eocene lacustrine clastic reservoirs in the Beibuwan Basin, South China Sea. *J. Pet. Sci. Eng.* **2016**, *146*, 1026−1036.

(12) Grafka, O.; Marynowski, L.; Simoneit, B. R. T. Phenyl derivatives of polycyclic aromatic compounds as indicators of hydrothermal activity in the Silurian black siliceous shales of the Bardzkie Mountains Poland. *Int. J. Coal Geol.* **2015**, *139*, 142−151.

(13) Hughes, W. B. Use of thiophenic organosulfur compounds in characterizing crude oils derived from carbonate versus siliciclastic sources. *AAPG Stud. Geol.* **1984**, *18*, 181−196.

(14) Douglas, A. G.; Mair, B. J. Sulfur: role in genesis of petroleum. *Science* **1965**, *147*, 499−501.

(15) Hanson, W. E. *Origin of petroleum*; Technology of Petroleum, 1960.

(16) Lu, H.; Shi, Q.; Lu, J.; Sheng, G.; Peng, P.'. A.; Hsu, C. S. Petroleum sulfur biomarkers analyzed by comprehensive two-

dimensional gas chromatography sulfur-specific detection and mass spectrometry. *Energy Fuels* **2013**, *27*, 7245−7251.
(17) Orr, W. L. Kerogen/asphaltene/sulfur relationships in sulfur-rich Monterey oils. *Org. Geochem.* **1986**, *10*, 499−516.
(18) Kropp, K. G.; Goncalves, J. A.; Andersson, J. T.; Fedorak, P. M. Bacterial transformations of benzothiophene and methylbenzothiophenes. *Environ. Sci. Technol.* **1994**, *28*, 1348−1356.
(19) Panda, S. K.; Arouri, K. R.; Hajji, A. A. Two dimensional LC and GC−MS: a combination toward the evaluation of potential geotracers in Saudi Arabian oil fields (Poster), Amsterdam, The Netherlands. *39th HPLC Conference on June*, 2013.
(20) Dai, L.; Li, S.; Lou, D.; Liu, X.; Suo, Y.; Yu, S. Numerical modeling of late Miocene tectonic inversion in the Xihu Sag, East China Sea Shelf Basin China. *J. Asian Earth Sci.* **2014**, *86*, 25−37.
(21) Li, C.; Li, S.; Xu, H. Petroleum geologic characteristics and exploration potential of middle−lower Eocene Baoshi Formation in the Xihu Sag. *Mar. Geol. Quat. Geol.* **2004**, *24*, 81−87.
(22) Li, S.; Li, C. Analysis on the petroleum resource distribution and exploration potential of the Xihu Depression, the East China Sea. *Pet. Geol. Exp.* **2003**, *25*, 721−728.
(23) Cheng, X.; Hou, D.; Zhou, X.; Liu, J.; Diao, H.; Jiang, Y.; Yu, Z. Organic geochemistry and kinetics for natural gas generation from mudstone and coal in the Xihu Sag, East China Sea Shelf Basin China. *Mar. Pet. Geol.* **2020**, *118*, No. 104405.
(24) Cheng, X.; Hou, D.; Zhao, Z.; Chen, X.; Diao, H. Sources of natural gases in the Xihu Sag, East China Sea Basin: Insights from stable carbon isotopes and confined system pyrolysis. *Energy Fuels* **2019**, *33*, 2166−2175.
(25) Su, A.; Chen, H.; Wang, C.; Li, P.; Zhang, H.; Xiong, W.; Lei, M. Genesis and maturity identification of oil and gas in the Xihu Sag, East China Sea Basin. *Pet. Explor. Dev.* **2013**, *40*, 558−565.
(26) Zhu, Y.; Li, Y.; Zhou, J.; Gu, S. Geochemical characteristics of Tertiary coal-bearing source rocks in Xihu depression, East China Sea basin. *Mar. Pet. Geol.* **2012**, *35*, 154−165.
(27) Tao, S.; Zou, C. Accumulation and distribution of natural gases in Xihu Sag, East China Sea Basin. *Pet. Explor. Dev.* **2005**, *32*, 103−110.
(28) Ye, J.; Qing, H.; Bend, S. L.; Gu, H. Petroleum systems in the offshore Xihu Basin on the continental shelf of the East China Sea. *AAPG Bull.* **2007**, *91*, 1167−1188.
(29) Yang, S.; Horsfield, B. Critical review of the uncertainty of Tmax in revealing the thermal maturity of organic matter in sedimentary rocks. *Int. J. Coal Geol.* **2020**, *225*, No. 103500.
(30) Huang, S.; Fang, X.; Liu, D.; Fang, C.; Huang, T. Natural gas genesis and sources in the Zizhou gas field, Ordos Basin China. *Int. J. Coal Geol.* **2015**, *152*, 132−143.
(31) Zou, C. N.; Yang, Z.; Tao, S. Z.; Yuan, X. J.; Zhu, R. K.; Hou, L. H.; Wu, S. T.; Sun, L.; Zhang, G. S.; Bai, B.; Wang, L.; Gao, X. H.; Pang, Z. L. Continuous hydrocarbon accumulation over a large area as a distinguishing characteristic of unconventional petroleum: the Ordos Basin, North−Central China. *Earth-Sci. Rev.* **2013**, *126*, 358−369.
(32) Dai, J.; Li, J.; Luo, X.; Zhang, W.; Hu, G.; Ma, C.; Guo, J.; Ge, S. Stable carbon isotope compositions and source rock geochemistry of the giant gas accumulations in the Ordos Basin China. *Org. Geochem.* **2005**, *36*, 1617−1635.
(33) Zhao, J.; Zhang, W.; Li, J.; Cao, Q.; Fan, Y. Genesis of tight sand gas in the Ordos Basin China. *Org. Geochem.* **2014**, *74*, 76−84.
(34) Guoyi, H.; Jin, L.; Xiuqin, S.; Zhongxi, H. The origin of natural gas and the hydrocarbon charging history of the Yulin gas field in the Ordos Basin China. *Int. J. Coal Geol.* **2010**, *81*, 381−391.
(35) He, Z.; Fu, J.; Xi, S.; Fu, S.; Bao, H. Geological features of reservoir formation of Sulige gas field. *Acta Pet. Sin.* **2003**, *24*, 6−12.
(36) Hanson, A. D.; Ritts, B. D.; Moldowan, J. M. Organic geochemistry of oil and source rock strata of the Ordos Basin, north-central China. *AAPG Bull.* **2007**, *91*, 1273−1293.
(37) Zhu, Z.; Li, M.; Li, J.; Qi, L.; Liu, X.; Xiao, H.; Leng, J. Identification, distribution and geochemical significance of dinaphthofurans in coals. *Org. Geochem.* **2022**, *166*, No. 104399.
(38) Zhu, Z.; Li, M.; Tang, Y.; Qi, L.; Leng, J.; Liu, X.; Xiao, H. Identification of phenyldibenzothiophenes in coals and the effects of thermal maturity on their distributions based on geochemical data and theoretical calculations. *Org. Geochem.* **2019**, *138*, No. 103910.
(39) Kilby, W. E. Recognition of vitrinite with non-uniaxial negative reflectance characteristics. *Int. J. Coal Geol.* **1988**, *9*, 267−285.
(40) Van den Dool, H.; Kratz, P. D. A generalization of the retention index system including linear temperature programmed gas-liquid partition chromatography. *J. Chromatogr. A* **1963**, *11*, 463−471.
(41) Kováts, E. Gas-chromatographische charakterisierung organischer verbindungen. Teil 1: Retentionsindices aliphatischer halogenide, alkohole, aldehyde und ketone. *Helv. Chim. Acta* **1958**, *41*, 1915−1932.
(42) Lee, M. L.; Vassilaros, D. L.; White, C. M. Retention indices for programmed-temperature capillary-column gas chromatography of polycyclic aromatic hydrocarbons. *Anal. Chem.* **1979**, *51*, 768−773.
(43) Liu, X.; Li, M.; Tang, Y.; Zhu, Z.; Qi, L.; Shi, S.; Leng, J.; Han, Q.; Xiao, H. Maturity indicators and its mechanism of triphenyls in sedimentary organic matter: Based on geochemical data and quantum chemical calculation. *Geochimica* **2020**, *49*, 218−226.
(44) Wang, N.; Li, M.; Liu, X.; Hong, H.; Tian, X.; Yang, C.; Shi, S.; Liu, P. Geo-chromatographic fractionation effect of methyldibenzofuran in dolomite reservoirs and its application in tracing oil filling pathways in the Sichuan Basin. *Mar. Pet. Geol.* **2020**, *113*, No. 104126.
(45) Xiao, H.; Li, M.; Wang, W.; You, B.; Liu, X.; Yang, Z.; Liu, J.; Chen, Q.; Uwiringiyimana, M. Identification, distribution and geochemical significance of four rearranged hopane series in crude oil. *Org. Geochem.* **2019**, *138*, No. 103929.
(46) Szczerba, M.; Rospondek, M. J. Controls on distributions of methylphenanthrenes in sedimentary rock extracts: Critical evaluation of existing geochemical data from molecular modelling. *Org. Geochem.* **2010**, *41*, 1297−1311.
(47) Li, M.; Liu, X.; Wang, T.-G.; Jiang, W.; Fang, R.; Yang, L.; Tang, Y. Fractionation of dibenzofurans during subsurface petroleum migration: Based on molecular dynamics simulation and reservoir geochemistry. *Org. Geochem.* **2018**, *115*, 220−232.
(48) Marynowski, L.; Rospondek, M. J.; Meyer Zu Reckendorf, R.; Simoneit, B. R. T. Phenyldibenzofurans and phenyldibenzothiophenes in marine sedimentary rocks and hydrothermal petroleum. *Org. Geochem.* **2002**, *33*, 701−714.
(49) Rospondek, M. J.; Marynowski, L.; Góra, M. Novel arylated polyaromatic thiophenes: Phenylnaphtho[*b*]thiophenes and naphthylbenzo[*b*]thiophenes as markers of organic matter diagenesis buffered by oxidising solutions. *Org. Geochem.* **2007**, *38*, 1729−1756.
(50) Rospondek, M. J.; Marynowski, L.; Chachaj, A.; Góra, M. Novel aryl polycyclic aromatic hydrocarbons: Phenylphenanthrene and phenylanthracene identification, occurrence and distribution in sedimentary rocks. *Org. Geochem.* **2009**, *40*, 986−1004.
(51) Rospondek, M. J.; Szczerba, M.; Malek, K.; Góra, M.; Marynowski, L. Comparison of phenyldibenzothiophene distributions predicted from molecular modelling with relevant experimental and geological data. *Org. Geochem.* **2008**, *39*, 1800−1815.
(52) Van Duin, A. C. T.; Baas, J. M. A.; van de Graaf, B.; de Leeuw, J. W.; Bastow, T. P.; Alexander, R. Comparison of calculated equilibrium mixtures of alkylnaphthalenes and alkylphenanthrenes with experimental and sedimentary data; the importance of entropy calculations. *Org. Geochem.* **1997**, *26*, 275−280.
(53) Yang, L.; Li, M.; Wang, T.-G.; Liu, X.; Jiang, W.; Fang, R.; Lai, H. Phenyldibenzofurans and methyldibenzofurans in source rocks and crude oils, and their implications for maturity and depositional environment. *Energy Fuels* **2017**, *31*, 2513−2523.
(54) Moldowan, J. M.; Peters, K. E. W. *The biomarker guide: Biomarkers and isotopes in petroleum systems and earth history*; Cambridge University Press: New York, 2005.
(55) Seifert, W. K.; Moldowan, J. M. The effect of thermal stress on source−rock quality as measured by hopane stereochemistry. *Phys. Chem. Earth* **1980**, *12*, 229−237.

https://doi.org/10.1021/acsearthspacechem.2c00309
ACS Earth Space Chem. XXXX, XXX, XXX−XXX

(56) Seifert, W. K.; Moldowan, J. M. Use of biological markers in petroleum exploration. *Methods Geochem. Geophys.* **1986**, *24*, 261−290.
(57) Peters, K. E.; Moldowan, J. M.; Sundararaman, P. Effects of hydrous pyrolysis on biomarker thermal maturity parameters: Monterey phosphatic and siliceous members. *Org. Geochem.* **1990**, *15*, 249−265.
(58) Kvalheim, O. M.; Christy, A. A.; Telnæs, N.; Bjørseth, A. Maturity determination of organic matter in coals using the methylphenanthrene distribution. *Geochim. Cosmochim. Acta* **1987**, *51*, 1883−1888.
(59) Radke, M. The methylphenanthrene index (MPI): A maturity parameter based on aromatic hydrocarbons. *Adv. Org. Geochem.* **1981**, *1983*, 504−512.
(60) Chakhmakhchev, A.; Suzuki, M.; Takayama, K. Distribution of alkylated dibenzothiophenes in petroleum as a tool for maturity assessments. *Org. Geochem.* **1997**, *26*, 483−489.
(61) Radke, M. Application of aromatic compounds as maturity indicators in source rocks and crude oils. *Mar. Pet. Geol.* **1988**, *5*, 224−236.
(62) Radke, M.; Welte, D. H.; Willsch, H. Maturity parameters based on aromatic hydrocarbons; influence of the organic matter type. *Org. Geochem.* **1986**, *10*, 51−63.
(63) Yang, S.; Li, M.; Liu, X.; Han, Q.; Wu, J.; Zhong, N. Thermodynamic stability of methyldibenzothiophenes in sedimentary rock extracts: Based on molecular simulation and geochemical data. *Org. Geochem.* **2019**, *129*, 24−41.
(64) Didyk, B. M.; Simoneit, B. R. T.; Brassell, S. C.; Eglinton, G. Organic geochemical indicators of palaeoenvironmental conditions of sedimentation. *Nature* **1978**, *272*, 216−222.
(65) Damsté, J. S. S.; Kenig, F.; Koopmans, M. P.; Köster, J.; Schouten, S.; Hayes, J. M.; De Leeuw, J. W. Evidence for gammacerane as an indicator of water column stratification. *Geochim. Cosmochim. Acta* **1995**, *59*, 1895−1900.
(66) Hughes, W. B.; Holba, A. G.; Dzou, L. I. P. The ratios of dibenzothiophene to phenanthrene and pristane to phytane as indicators of depositional environment and lithology of petroleum source rocks. *Geochim. Cosmochim. Acta* **1995**, *59*, 3581−3598.
(67) Li, M.; Ellis, G. S. Qualitative and quantitative analysis of dibenzofuran, alkyldibenzofurans, and benzo[*b*]naphthofurans in crude oils and source rock extracts. *Energy Fuels* **2015**, *29*, 1421−1430.
(68) Radke, M.; Vriend, S. P.; Ramanampisoa, L. R. Alkyldibenzofurans in terrestrial rocks: influence of organic facies and maturation. *Geochim. Cosmochim. Acta* **2000**, *64*, 275−286.

https://doi.org/10.1021/acsearthspacechem.2c00309
ACS Earth Space Chem. XXXX, XXX, XXX−XXX